



Computational approaches for the design of novel dopamine D₂ and serotonin 5-HT_{2A} receptor dual antagonist towards schizophrenia

Akash Rathore¹ · Vivek Asati² · Mitali Mishra¹ · Ratnesh Das³ · Varsha Kashaw⁴ · Sushil Kumar Kashaw¹

Received: 27 April 2021 / Accepted: 3 February 2022

© The Author(s), under exclusive licence to Springer-Verlag GmbH Germany, part of Springer Nature 2022

Abstract

Piperidine and piperazine derivatives exhibit a diverse range of biological applications, including antipsychotic activity. In this study, a dataset of molecules containing piperidine, piperazine moieties that possess serotonin 5-HT_{2A} and dopamine D₂ inhibitory activity have been chosen for Pharmacophore modeling, Quantitative Structure–Activity (3D-QSAR) Relationship, Molecular docking, and ADME studies. The pharmacophoric hypothesis was found to be AAHPRRR_1 having seven features as one H-bond acceptor (A), one hydrophobic (H), one positive ion acceptor (P), and three aromatic rings (R), with survival score = 6.465 and AUC = 0.92. Based on the best hypothesis, the ZINC-Data base was virtually screened to find out the lead molecules. 3D-QSAR model, including internal and external validation showed comparative molecular field analysis (CoMFA) against 5HT_{2A} ($q^2=0.552$, $R^2=0.889$, and r^2 poured. = 0.653 and number of component 5) and comparative molecular similarity indices analysis (CoMSIA) ($q^2=0.599$, $R^2=0.893$, and r^2 pred. = 0.617), for D₂ (CoMFA, $q^2=0.577$, $R^2=0.863$, and r^2 pred. = 0.598) (CoMSIA, $q^2=0.532$, $R^2=0.82$) all results exhibited better productivity and significant statistical reliability of the model. The docking study was carried out on the crystal structure of 5-HT_{2A} having PDB ID; 6A93 and D₂ receptor having PDB ID; 6CM4. The screened compound ZINC74289318 possess a higher docking score – 10.744 and – 11.388 than co-crystallized ligand docking score – 8.840 and – 10.06 against 5-HT_{2A} and D₂ receptor respectively. Further, ZINC74289318 was screened for all drug-likeness parameters and no showed violation of the Lipinski rule of five. Also, it was found to possess good bioavailability of 0.55 with synthetic accessibility of 4.42 which is greater than risperidone.

Keywords Piperidine and piperazine · 5-HT_{2A} and dopamine D₂ inhibitors · 3D-QSAR model · CoMFA · CoMSIA

Introduction

Schizophrenia is a chronic and severe neuropsychiatric disorder affecting about 1% of the world's population (Rossler et al. 2005). The adolescence or early adulthood persons facing some brain hormonal imbalance, viral infection, error in

genetic encoding as well as stressful environmental factors are more susceptible to develop symptoms of schizophrenia. Uncontrolled behavior, disruption in thinking, hallucination, perception, sense of self, isolation, hearing voices delusion are the major symptoms of schizophrenia (Liddle 1987; McCutcheon et al. 2020).

Antipsychotic drugs are the initial therapeutic intervention for schizophrenia. The pathophysiology of disease and medication has yet to be clearly defined. The development of antipsychotic drugs in recent decades has been extremely influenced by the dopamine hypothesis, regulated by dopamine pathways in a different area of the brain that includes mesolimbic and mesocortical pathways (Leucht et al. 2009; Cao et al. 2018). Typical antipsychotics (eg. haloperidol, clozapine, chlorpromazine) are potent inhibitors of dopamine D₂ receptor in the mid striatum region of the brain, which block the mesolimbic and nigrostriatal dopamine circuit and reduce the positive symptoms of schizophrenia

✉ Sushil Kumar Kashaw
sushilkashaw@gmail.com

¹ Department of Pharmaceutical Sciences, Dr. Harisingh Gour University (A Central University), Sagar, Madhya Pradesh 470003, India

² Department of Pharmaceutical Chemistry, ISF College of Pharmacy, Moga, Punjab, India

³ Department of Chemistry, Dr. Harisingh Gour University (A Central University), Sagar, Madhya Pradesh, India

⁴ Sagar Institute of Pharmaceutical Sciences, Sagar, Madhya Pradesh, India

followed by severe side effects including acute Parkinson's, dyskinesia, common side effect includes extrapyramidal symptoms (Kapur 2001; Peprah et al. 2012). Typical antipsychotics treat positive symptoms, but medical treatment for the negative and cognitive disorders is an urgent need and still challenging for researchers. The atypical antipsychotic having a broad antipsychotic mechanism of action, but due to off-target binding, it produces undesirable side effects such as hyperglycemia, hyperprolactinemia, QT prolongation, and weight gain (Huang et al. 2015; Butini et al. 2008). Medical research is urgently required to develop new antipsychotic drugs that can effectively control positive, negative, and cognitive symptoms of schizophrenia with reduced major and minor harmful side effects (Xiamuxi et al. 2017).

Dopamine D_2 and serotonin 5-HT_{2A} both are high-affinity G-protein coupled receptors and crucial targets for the treatment of schizophrenia. These receptors, involved in the pathophysiology of many neuropsychiatric disorders like Parkinson's, anxiety, and depression (Xu et al. 2018). Serotonin 5-HT_{2A} receptor regulates and manages negative and cognitive impairment symptoms. Many studies have been reported that in combination antagonist effect on D_2 and 5-HT_{2A} receptor can improve, negative and cognitive symptoms and reduces side effects. Furthermore tandospirone, aripiprazole is newer atypical antipsychotic causes, partial agonism of 5-HT_{1A} receptor, and improve the cognitive decline in schizophrenic patients. 5-HT_{1A} receptor activation also contributes to the antianxiety properties of antipsychotic (Modugula and Kumar 2020; Kumar et al. 2018).

Zajdel et al., used novel azinesulfonamides of cyclic amine skeleton against D_2R partial agonism/antagonism and 5-HT_{2A} , $5\text{-HT}_{6/7}$ antagonism action, to reduced positive and negative symptoms with minimum side effects. Currently, compound **18 g** has been tested in male Wistar rats, and it showed excellent in vitro and in vivo efficacy in a pre-clinical model of schizophrenia with the addition of a good pharmacokinetic profile (Zajdel et al. 2018). There are no comprehensive and theoretical studies that have shown the structure–activity relationship. To promote D_2 and 5-HT_{2A} receptor antagonist activity, we explored molecular modeling studies for the treatment of schizophrenia. In this study, we investigated a systematic study of azine sulfonamide derivatives as a dual D_2 and 5-HT_{2A} receptors antagonist and focused on the structure-based drug design methods like pharmacophore modeling, 3D-QSAR, molecular docking. Further, molecules were subjected to ADME studies. A molecular library was built based on docking and pharmacophore hypothesis for D_2 and 5-HT_{2A} receptor inhibitory activity. This study provides the rationale to future scientists for the development of novel D_2 and 5-HT_{2A} receptors antagonist as antipsychotic agents with fewer side effects and high tolerability.

Material and methods

Software used

The three-dimensional (3D) structures of compounds were sketched using Chem-Draw ultra 12.0 and saved in (.mol extension) files. The pharmacophore modeling, molecular docking, and virtual screening studies were performed using Schrodinger software, 3D-QSAR (CoMFA, CoMSIA) studies performed by SYBYL-X-2.1.1 software and for ADME the online utilities Swiss ADME prediction tool were used to determine pharmacokinetic parameters of compounds (Zhang, et al. 2020).

Data set

Dataset of 45 compounds was taken for computational studies, possessing dual antagonists' activity for D_2 and 5-HT_{2A} receptors, and used to develop the In-silico models (Zajdel et al. 2018). Pharmacophore modeling and CoMFA, CoMSIA studies of the 3D-QSAR were done using the different diverse activity of training and test set for dual targets. The given activity K_i (nM) values were converted into pK_i (nM) to build the statistical model (Ghasemi and Shiri 2012; Abdizadeh et al. 2020).

Molecular structure and biological activity of test set and training set compounds given in Table 1 with their predicted model's activity using CoMFA, CoMSIA descriptor. 3D-QSAR models were generated using training and test set compounds of both the targets.

Pharmacophore modeling

The LigPrep module of Schrödinger software was used to convert the 2D structure to 3D and minimized the energy using OPLS_2005 force field with root mean square deviation (RMSD) cut-off of 0.01 Å. The resulting lowest energy-bearing stable conformers were used for pharmacophore modeling (Dixon et al. 2006). These prepared ligands were used in the phase module of software (v5.2) to build a pharmacophore model. The ligands were then assigned as active and inactive with a threshold of $pK_i \geq 8.522$ nM (actives) and $pK_i \leq 6.528$ nM (inactive), remaining compounds assigned as moderate actives. However, 11 molecules were found to be active and 7 molecules were found to be inactive. The phase has been a proven tool for flexible ligand alignment (Rajeswari et al. 2014; Lee et al. 2018). So, the 45 compounds of the data set were aligned using the best finding common core method of phase (Fig. 1).

The PHASE were built in six different pharmacophoric features such as hydrophobic group (H), hydrogen bond acceptor (A), hydrogen bond donor (D), positively ionizable

Table 1 Actual and predicted pK_i (nM) values for CoMFA and CoMSIA based 3D-QSAR model (PLS analysis)

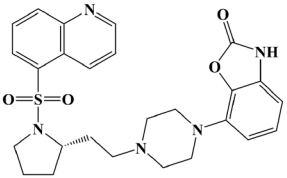
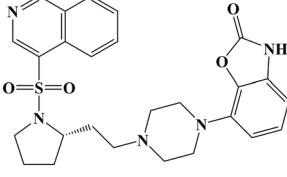
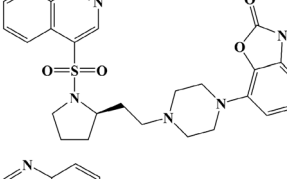
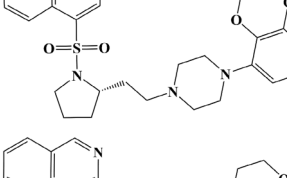
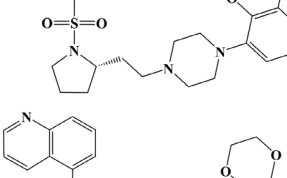
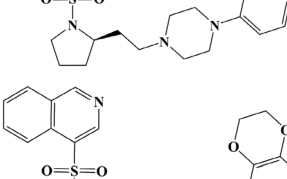
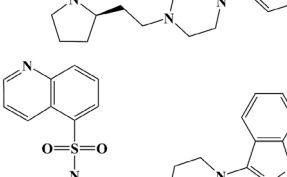
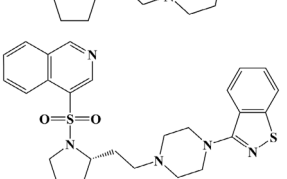

No. ^y	Name	Compound structure	Actual pK_i		Predicted pK_i			
			5-HT _{2A} R ^a	D ₂ R ^b	CoMFA ^a	CoMSIA ^a	CoMFA ^b	CoMSIA ^b
1	1 g		5.853	8.045	–	–	–	–
2	2 g		5.690	8.301	–	–	8.3692	8.4439
3	3 g		5.705	7.920	–	–	–	–
4	4 g		6.958	7.886	6.9512	6.8323	7.8899	7.5448
5	5 g		7.040	7.721	7.0601	7.0686	7.6973	7.7359
6	6 g		6.528*	7.920	7.259	7.1362	7.9603	7.8885
7	7 g		6.408	7.657	6.3359	6.44	–	–
8	8 g		7.795	9	7.5777	7.5894	9.2965	9.2269
9	9 g		7.886*	9.853	7.9126	7.8631	9.4775	9.3797

Table 1 (continued)

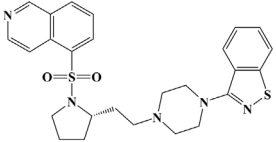
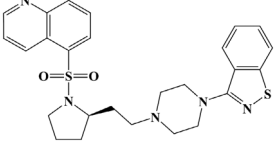
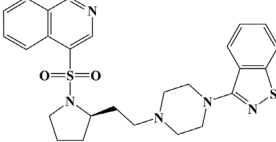
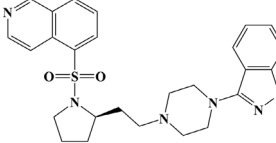
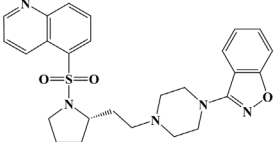
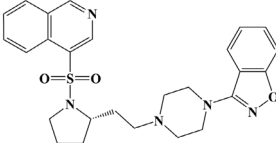
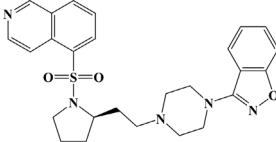
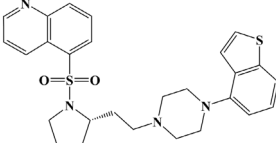
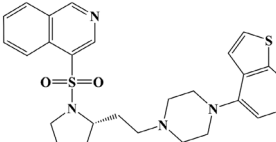
No. ^y	Name	Compound structure	Actual pK_i		Predicted pK_i			
			5-HT _{2A} R ^a	D ₂ R ^b	CoMFA ^a	CoMSIA ^a	CoMFA ^b	CoMSIA ^b
10	10 g		7.744	9.301	7.8749	7.7775	9.3739	9.2745
11	11 g		7.677	9.154	7.5285	7.5888	8.3432	8.3389
12	12 g		8	9.045	7.9126	7.8631	9.4775	9.3797
13	13 g		7.823	9.522	7.8749	7.7775	9.3739	9.2745
14	14 g		7.309	8.397 [^]	7.4447	7.6072	9.322	9.3139
15	15 g		7.481	8.522 [^]	7.4003	7.6328	9.4784	9.4604
16	16 g		7.387 [*]	8.522	7.9961	8.0611	9.4578	9.3541
17	17 g		7.443	7.795	7.4754	7.6491	7.9256	8.0091
18	18 g		8.045 [*]	7.958	7.3872	7.3826	8.0656	8.2388

Table 1 (continued)

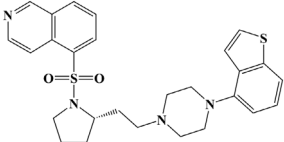
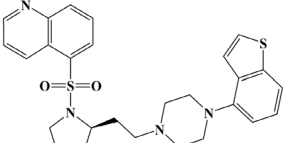
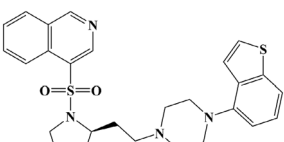
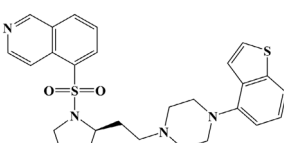
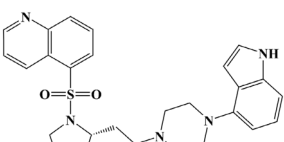
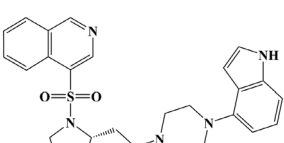
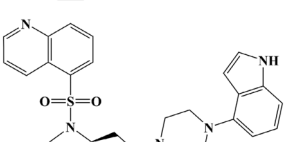
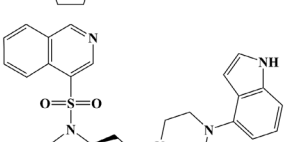
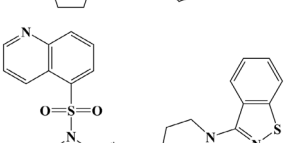
No. ^y	Name	Compound structure	Actual pK_i		Predicted pK_i			
			5-HT _{2A} R ^a	D ₂ R ^b	CoMFA ^a	CoMSIA ^a	CoMFA ^b	CoMSIA ^b
19	19 g		8.045	8.301 [^]	8.1835	7.9693	8.2251	8.1343
20	20 g		7.251	8.397 [^]	7.5427	7.6695	7.9709	7.9997
21	21 g		7.585	8.221	7.6313	7.4526	8.237	8.3663
22	22 g		7.721	8.301 [^]	7.8205	7.8702	9.0928	8.7064
23	23 g		6.612	7.376	6.7073	6.5121	–	–
24	24 g		7.086	7.431	7.0829	6.9737	–	–
25	25 g		6.345	8.096	6.7073	6.5121	8.0796	7.9788
26	26 g		7.119	8.522	7.1672	7.1559	8.2085	8.2203
27	27 g		7.522	7.958	7.5285	7.5888	8.3432	8.3389

Table 1 (continued)

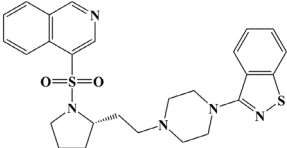
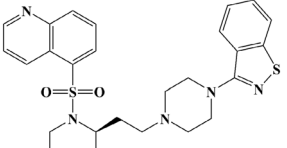
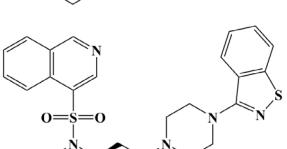
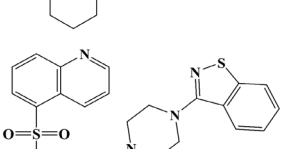
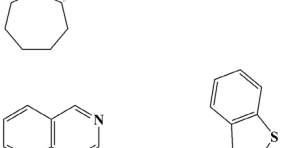
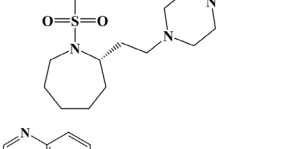
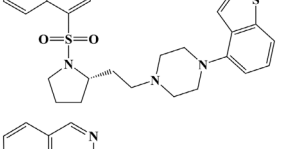
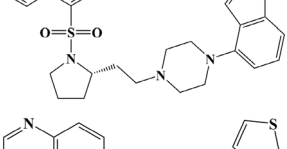
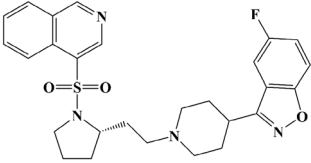
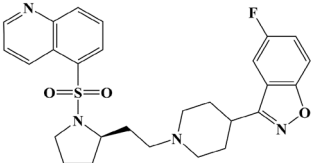
No. ^y	Name	Compound structure	Actual pK_i		Predicted pK_i			
			5-HT _{2A} R ^a	D ₂ R ^b	CoMFA ^a	CoMSIA ^a	CoMFA ^b	CoMSIA ^b
28	28 g		7.619	8	7.473	7.5407	8.0867	8.3262
29	29 g		7.537	8.154 [^]	7.6166	7.4884	8.3636	8.6387
30	30 g		7.455	8.301	7.4666	7.554	8.4198	8.5494
31	31 g		7.522	8.397	7.5353	7.4365	8.3455	8.2844
32	32 g		7.585 [*]	8.522	7.4164	7.1331	8.4966	8.6317
33	33 g		8.154	7.619	7.5191	7.6628	–	–
34	34 g		7.795	7.537	7.7409	7.8029	–	–
35	35 g		7.455 [*]	7.677	7.3406	7.4202	–	–

Table 1 (continued)

No. ^y	Name	Compound structure	Actual pK_i		Predicted pK_i			
			5-HT _{2A} R ^a	D ₂ R ^b	CoMFA ^a	CoMSIA ^a	CoMFA ^b	CoMSIA ^b
36	36 g		7.193	7.638	7.2043	7.3247	–	–
37	37 g		7.292*	8	7.9534	7.6951	8.0071	7.8901
38	38 g		7.537	8.221^	7.5452	7.4651	8.0079	7.9523
39	1 h		5.853	7.958	–	–	–	–
40	2 h		6.623	7.886	6.4871	6.6411	7.9108	7.9601
41	3 h		5.939	7.823^	–	–	8.3619	8.6086
42	4 h		5.720	7.920	–	–	7.9108	7.9601
43	5 h		7.920*	8.7695	8.2763	8.2379	8.8371	8.8623

Table 1 (continued)

No. ^y	Name	Compound structure	Actual pK_i		Predicted pK_i			
			5-HT _{2A} R ^a	D ₂ R ^b	CoMFA ^a	CoMSIA ^a	CoMFA ^b	CoMSIA ^b
44	6 h		8.221	10	8.2691	8.2563	9.7896	9.7933
45	7 h		8.301	8.698	8.2763	8.2379	8.8371	8.8623

*Test set in case of 5-HT_{2A}R

^aModel constructed with pK_i value of 5-HT_{2A}R antagonists

^bModel constructed with pK_i value of D₂R antagonists; ^Test set in case of D₂R

–Model specific, unpredicted biological activity

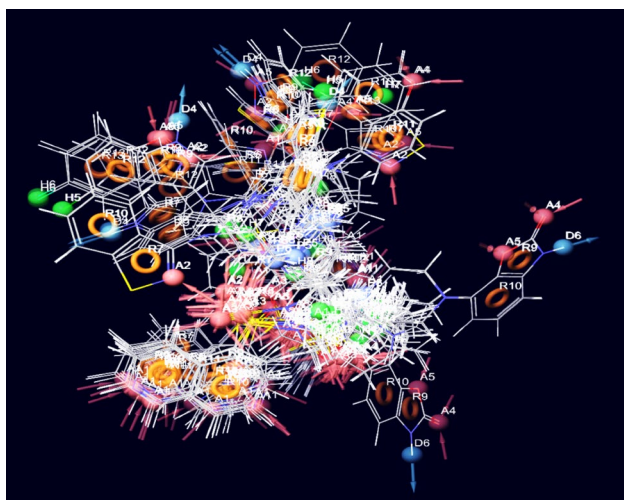


Fig. 1 Alignment of the molecule to detect common pharmacophore

(P), negatively ionizable (N), and ring aromaticity (R). The maximum pharmacophore feature or sites was set up to 7 and minimum up to 4 which generate different pharmacophore hypothesis (Wood, et al. 2012). The generated hypotheses were ranked automatically based on Phase Hypo Scores, survival scores, vector scores, site score, volume score, inactive score, selectivity scores, and values of area under the curve (AUC) of receiver operating curve (ROC) (Table 2). Among all developed pharmacophore hypotheses the best hypothesis showed 7 common features with similarity in spatial arrangements of active ligands. The hypothesis has seven features: two hydrogen bond acceptors, one hydrogen bond donor, one positive ion acceptor, and three-ring

features (AAHPRRR-1) selected as the best hypothesis model (Fig. 2). The distance and angle between pharmacophore features of the best pharmacophore model were given in Tables 3 and 4 respectively.

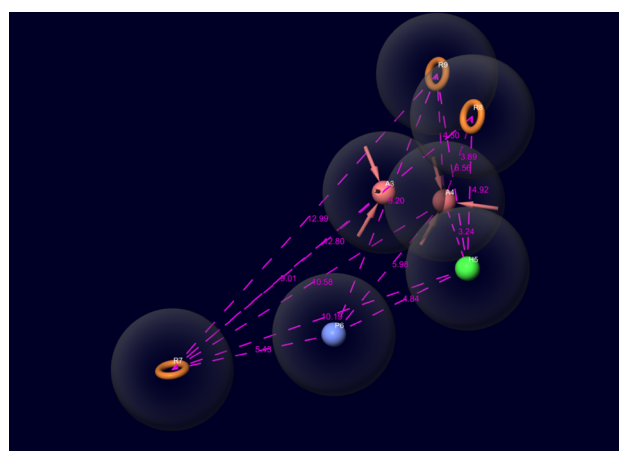
A tree-based separating approach has been used for the generation of pharmacophore. The groups that are similar to their inter-site distance i.e., site-to-site distances in the common pharmacophore aligned with all 45 compounds. The active pharmacophore model generated essential features for receptor affinity.

Identification of antipsychotics drugs through virtual screening

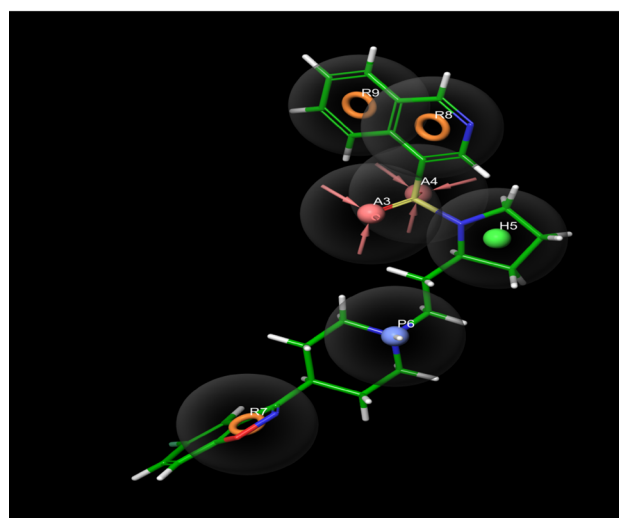
The best pharmacophore hypothesis (AAHPRRR_1) was used as a template for the virtual screening of molecules from the ZINC database. The virtual screening, selected only those compounds having similar chemical features to that template. Among the selected compounds, some are similar to the active compound of the data set and some are novel. The total 40,000 compounds were filtered through fitness scores and matched to hypothesis; among them, 4000 compounds were passed. Further, these compounds were screened through drug-likeness criteria followed by the Lipinski rule of five. Finally, the filtered compounds were used for docking studies using HTVS, SP, and XP methods of docking, and based on their docking results lead molecules were chosen (Jaiteh, et al. 2020).

Table 2 Pharmacophore hypotheses derived by PHASE

Sr. no	Hypothesis	Phase hypo score	BEDROC score	Survival scores	Inactive Score	Site score	Vector Score	Volume score	Selectivity	AUC
1	AAHPRRR_1	1.25	0.95	6.465	1.361	0.739	1.0	0.81	3.87	0.92
2	AHPRRR_1	1.21	0.95	5.832	1.37	0.75	1.0	0.81	3.22	0.92
3	AHPRRR_3	1.19	0.88	5.75	1.49	0.71	1.0	0.81	3.19	0.92
4	APRRR_1	1.16	0.94	5.03	1.35	0.74	1.0	0.81	2.44	0.92
5	HPRRR_1	1.16	0.86	5.21	1.37	0.76	1.0	0.81	2.59	0.92
6	HPRRR_3	1.15	0.90	5.13	1.45	0.72	1.0	0.78	2.58	0.92
7	HPRR_5	1.13	0.95	5.06	1.34	0.66	1.0	0.77	2.58	0.91
8	PRRR_3	1.1	0.75	4.47	1.53	0.76	1.0	0.77	1.89	0.91
10	HPRR_4	1.07	0.59	4.46	1.44	0.80	1.0	0.79	1.82	0.91



(a)



(b)

Fig. 2 **a** The pharmacophore model (AAHPRRR_1) generated by PHASE. The model illustrates acceptor feature (AA; pinkish red-coloured arrows), hydrophobic (H: green coloured) and aromatic ring (R: brown coloured features), positively ionizable (P: sky blue coloured); **b** Pharmacophore model of most active compound 6 h

3D-QSAR model generation

The 3D models were generated using diverse range activity of D_2 and 5-HT_{2A} receptor inhibitors. In this present study, the energies of electrostatic and steric fields were calculated based on CoMFA and CoMSIA models, by using Sp^3 carbon atom with a Van der Waals force radius of 1.5 \AA charge of $+1.0$ and attenuation factor 0.1 to 0.3 \AA , including five fields hydrophobic, hydrogen bond donor and hydrogen bond acceptor, steric and electrostatic, with probe atom charge $+1$ each lattice, radius of 1 \AA (Klebe et al. 1994; Murthy and Kulkarni 2002). The 3D-QSAR model was developed to investigate the structural features and biological activity of molecules. In the case of $5\text{-HT}_{2A}R$ and D_2R , a total of 45

Table 3 The distance measured between two sites

Site1	Site2	Distance
H5	R8	4.92
	A3	3.72
	A4	3.24
	R9	6.56
	R7	10.19
R7	H5	10.19
	A3	9.01
	A4	10.58
	R9	12.99
	R8	12.80
P6	R7	5.43
	H5	4.84
	A3	4.91
	A4	5.98
	R8	8.37
R9	R9	9.20
	R9	2.45
	A4	3.89
R8	A3	3.89
	A3	4.30
R9	A4	4.30
	A3	4.30
A3	A4	2.56

Table 4 Angles between different sites of the pharmacophore model

Site1	Site2	Site3	Angle
R7	P6	A3	121.3
R7	A3	P6	31.1
P6	H5	A3	68.6
P6	H5	A4	93.3
R8	R9	A3	63.5
R8	A3	R9	34.4
A4	R8	R9	82.1
H5	A3	P6	66.6
R8	H5	R7	111
R7	R9	H5	50.7
R7	R8	R9	88.9
R9	A4	R8	34.4
H5	A3	R8	80.5
P6	H5	R9	106.7
P6	R8	R7	17.4
R8	P6	A4	25.0
A3	R8	R9	82.1

compounds were taken for model development of which 78% of compounds were taken as training sets and 22% compounds as the test set. The best 3D-QSAR model with its statistical values is reported in Table 5. The actual and predicted biological activities (pK_i) of molecules, calculated by

Table 5 Statistical parameter of the developed 3D-QSAR models

Parameters	COMFA ^a	COMSIA ^a	COMFA ^b	COMSIA ^b
Q^2 (LOO)	0.552	0.599	0.577	0.532
R^2	0.889	0.893	0.863	0.820
R^2_{CV}	0.565	0.605	0.582	0.549
SEE	0.1836	0.1843	0.253	0.296
NOC	5	6	2	3
F Value	207.423	192.325	210.584	186.246
SEE _{BS}	0.163	0.133	0.193	0.263
R^2_{BS}	0.894	0.942	0.916	0.843
SD _{BS}	0.075	0.023	0.063	0.076
Field contribution				
Steric	–	0.03	–	0.25
Electrostatic	–	5.54	–	0.63
Hydrophobic	–	1.49	–	2.09
Donor	–	0.00	–	1.15
Acceptor	–	1.07	–	1.24

^aModel constructed with pK_i value of 5-HT_{2A}R antagonists; ^bModel constructed with pK_i value of D₂R antagonists. NOC is the optimum number of component, q^2 is leave-one-out (LOO) correlation coefficient, r^2 non-cross validation coefficient, r^2_{cv} is re-cross validation coefficient, standard error of estimate (SEE), F is the F-train value, r^2_{bs} is mean r^2 of bootstrapping analysis, SEE_{bs} standard error of estimation of bootstrapping analysis, SD_{bs} is mean standard deviation by bootstrapping analysis

using CoMFA and CoMSIA models of 3D-QSAR study, for both the (5-HT_{2A} and D₂) target were reported in Table 1.

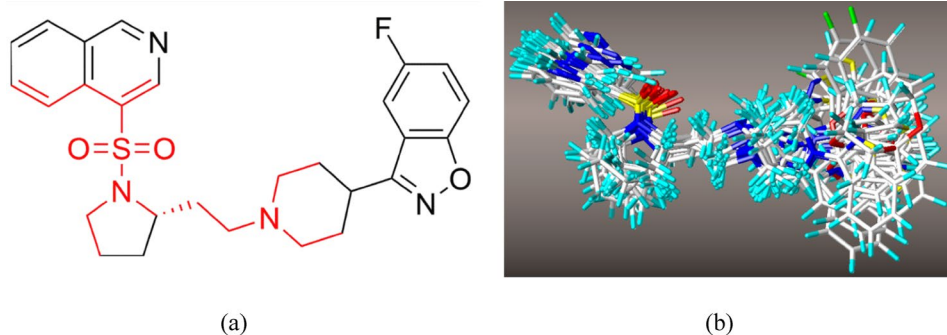
Energy minimization and alignment

Best stable conformers of compounds were generated by minimizing the energy which is a very crucial step for the model development. All the compounds were imported in the SYBYL window (molecular area) and operated through the Powell method at 0.05 kcal/(mol*Å) termination gradient, maximum iteration count 10,000, Gasteiger-Huckel as force field tripos charges, dielectric constant 1.00, RMS displacement 0.001 with initial optimization simplex. The molecular alignment of compounds was done with distil rigid alignment method which automatically finds the common core for alignment of the molecule (Ghaleb, et al. 2017; Oprea et al. 2001). The most potent compound 6 h was used as a core molecule for alignment (Fig. 3).

PLS analysis and QSAR model validation

PLS analysis is a technique derived to analyze complex structural data and perform linear regression between the molecular descriptors (independent variables) and biological activity (dependent variable). The validation of QSAR models was done using internal or external validation parameters

Fig. 3 Compound 6 h **a** Common core skeleton is shown in red. **b** Structure-based alignment of data set molecules



to estimate the predictive ability of models. To evaluate the model's predictive ability and robustness the following criteria must be followed, the cross-validation coefficient ($q^2 > 0.5$), correlation of coefficient ($r^2 > 0.5$), Standard error of estimate ($SEE < 0.3$), number of components ($N > 20$). Further, cross-validation of models was also checked by calculating r^2_{cv} (re-cross validation coefficient), r^2_{bs} (mean r^2 of bootstrapping analysis), SEE_{bs} (standard error of estimation of bootstrapping analysis), and SD_{bs} (mean standard deviation of bootstrapping analysis) (Verma et al. 2010).

Molecular docking

Docking studies were performed by Glide module V5.2 of Schrödinger software. The crystal structures of 5-HT_{2A} and D₂ receptors were fetched from the RCSB protein data bank (<http://www.rcsb.org/>), having PDB ID: D₂ (6CM4); 5-HT_{2A} (6A93) (Kimura, et al. 2019; Wang et al. 2018). Both the target proteins were pre-processed by adding hydrogen atoms, removing water molecules except essential ones, removing side chains break, removing unnecessary ligands other than reference ligands, and finally, the energy of the protein molecules was minimized. Before operating the docking procedure, the grid was generated by mapping the active site, possessing a co-crystallized ligand (risperidone), and exploring the binding interactions. The final ligands were screened based on their docking scores, energies, and molecular interactions with amino acid residues.

Molecular ADMET prediction and Lipinski's rule for drug likeliness

The *in-silico* tools predicting ADMET parameters and drug-likeness profile for the preliminary estimation of the physicochemical, pharmacokinetic, and drug-like parameters in drug discovery. This study provides direction to access pharmacokinetic parameters (Adsorption, Distribution, Metabolism, Excretion, and Toxicity; ADMET). The rule access to filter compounds and drug-likeness character is based on Lipinski rule of five and the synthetic accessibility problematic scale was 1–10.

The Swiss ADMET web tool is used for the presented study, is freely accessible at <http://www.swissadme.ch> and run as user friendly and results, analysis is easy to understand and estimate the pharmacokinetic parameters of ADMET (Daina et al. 2017).

In the present study, ADMET studies of all compounds were performed by online SwissADME software. The model's results were explained in terms of different pharmacokinetic parameters such as drug-likeness, Lipinski's rule of five, GI absorption, blood–brain permeability, solubility, enzyme inhibition, octanol/water partition coefficient. The SwissADME is a tool to predict numerous biological system conditions hypothetically. The cytochrome profiling of these compounds was also predicted by *in silico* SwissADME tool.

Results and discussion

Pharmacophore model analysis

The common pharmacophore model was evaluated with a survival score of 6.46, site score of 0.739, selectivity score of 3.87, and survival inactive score of 1.361. The model was further validated through the accuracy of the test measured by the AUC and ROC curve. The value of AUC signified the accuracy of the model ($AUC > 0.9$ indicated high accuracy of the model, while values in between 0.5 to 0.7 showed moderate model and for poor model $AUC = 0.5$). The AUC of the developed model is 0.92 (Table 2) showed that the predicted pharmacophore model is very significant and accurate. The features of developed hypotheses are essential for receptor-ligand interactions. The distances and angles between these features are crucial to measuring the active sites of the pharmacophore mapping model. (Tables 3, 4).

The specificity and sensitivity of the model are determined by the ROC plot having specificity at the X-axis and sensitivity at the Y-axis. This plot also distinguishes active and inactive compounds present in the data set (Fig. 4).

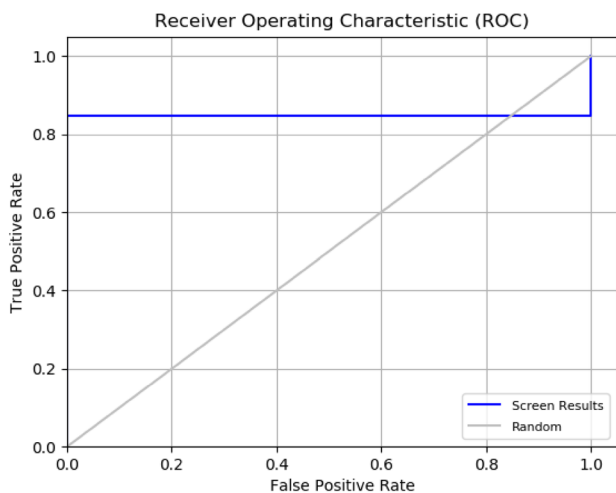


Fig. 4 Receiver operating curve of (AAHPRRR_1) developed model

3D-QSAR models analysis

In this study, CoMFA and CoMSIA models were built and evaluated successfully. The statistical parameter of models is presented in Table 5. The PLS analysis of CoMSIA^a showed the optimal number of component (ONC) of 6 and Q^2 value of 0.599, while a non-cross-validated R^2 value is 0.893, F value of 192.325, and standard error of estimate 0.1843. The cross-validation coefficient (Q^2) was checked by a cross-validated correlation coefficient (R^2_{cv}) value of 0.565. The

model accuracy and robustness were further determined by bootstrapping analysis of the CoMSIA^a model, which showed R^2_{bs} 0.894, SD_{bs} 0.075, and SEE_{bs} 0.163. The percentage contribution of a steric, electrostatic, hydrophobic, donor, and acceptor of the CoMSIA^a model were 0.03%, 5.54%, 1.49, 0.00, and 1.07% respectively.

In the case of the CoMSIA^b model, the PLS analysis of the model showed the cross-validation coefficient of 0.532 with three components. The non-cross-validated PLS analysis results in conventional R^2 0.820, standard error of estimate 0.296. Further, validation of the model is carried out by estimating R^2_{cv} is 0.582, F value is 186.24, R^2_{bs} 0.843, and SD_{bs} is 0.076. The steric field contribution of the CoMSIA^b model found to be lower than electrostatic, hydrophobic, H-bond donor, and acceptor was given in Table 5.

The experimental and predicted activity values are shown in Table 1, based on these values a scatter plot is deduced and represented in Fig. 5A for (CoMSIA^a) and Fig. 5B for (CoMSIA^b).

3D-QSAR contour map analysis

The best contour map of the CoMFA and CoMSIA model was graphically interpreted. The contour map was shown with the most active compound **6 h** of the dataset to find out the structure–activity relationship among all compounds.

The results from steric and electrostatic contour maps of the CoMFA model were found to be similar to the steric,

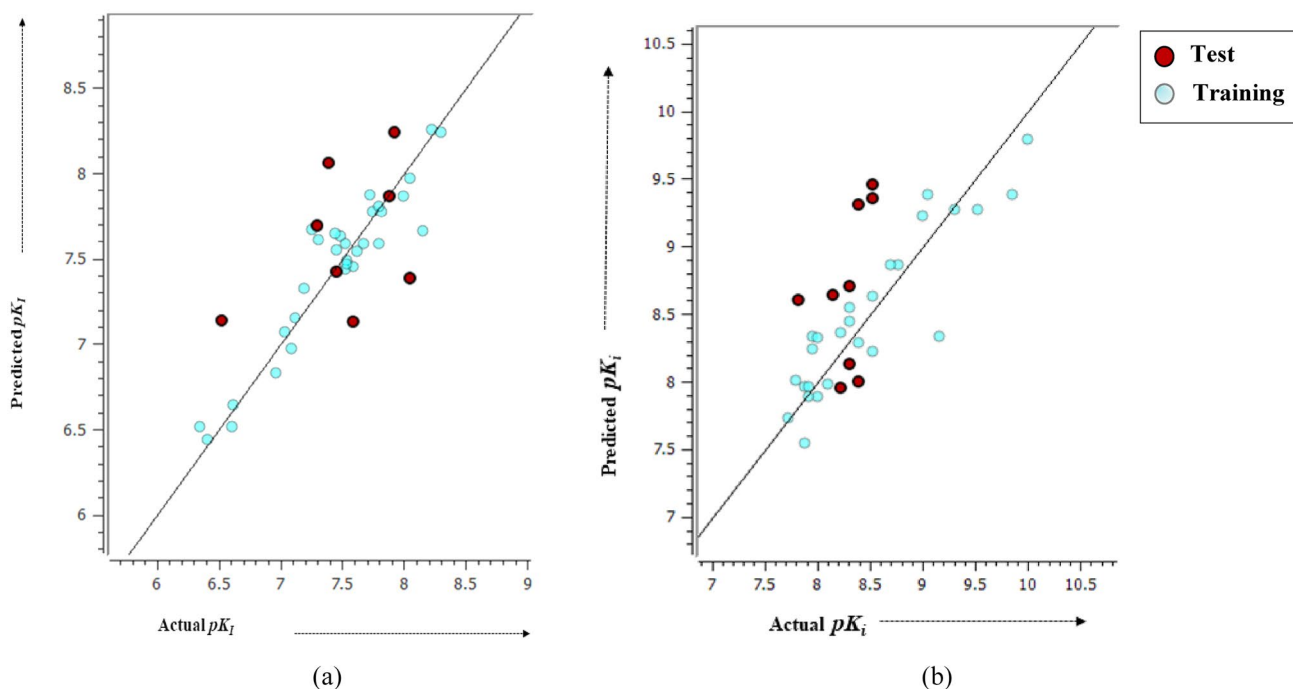


Fig. 5 Plots of correlation of predicted versus actual pK_i values based on (a). CoMSIA^a, b CoMSIA^b models

and electrostatic contour maps of the CoMSIA model. The steric, electrostatic, hydrophobic, H-bond donor and acceptor contour maps resulted from the CoMSIA^a and CoMSIA^b model of 5-HT_{2A} and D₂ receptor activities, are shown in Figs. 6 and 7 respectively. In Fig. 6a, as the presence of steric field (green regions) are found to be favorable for bulky groups which can enhance the antagonist activity, while the yellow color contour map has shown sterically unfavorable region which means bulky substitutions on this position lead to decrease the receptor activity. Benzo-ring of benzo-(d) isoxazole moiety suggested that the presence of steric bulk around benzene ring may enhance the activity, but a little yellow polyhedral contour near the five-membered ring of benz-isoxazole moiety suggested that the absence of steric bulk is desired for receptor activity. In the case of the electrostatic field CoMSIA^a model, the blue contour (b) regions of the respective molecule showed that the presence of positively charged groups would improve the

activity of compounds. While red contours present near the 6th position of isoquinoline and covered with isoxazole five-membered ring of benzo[d]isoxazole moiety, suggested that the addition of electronegative groups in these regions are favorable for biological activity. The hydrophobic contour (c) near the 6th and 7th positions of isoquinoline moiety suggested that the presence of hydrophobic groups in this region may decrease the receptor activity. The hydrophobic contour designated with white color suggested that substitution of hydrophobic groups at the 6th and 7th position of isoquinoline may decrease the receptor activity shown in Fig. 6c. While yellow indicated that the presence of hydrophobic groups in this region enhanced the activity of the compound. The magenta contour of Fig. 6d showed that the presence of H-bond acceptor groups in these regions increases the activity of the compound, while the red color indicated that the presence of H-bond acceptor groups is unfavorable for the bioactivity of compounds.

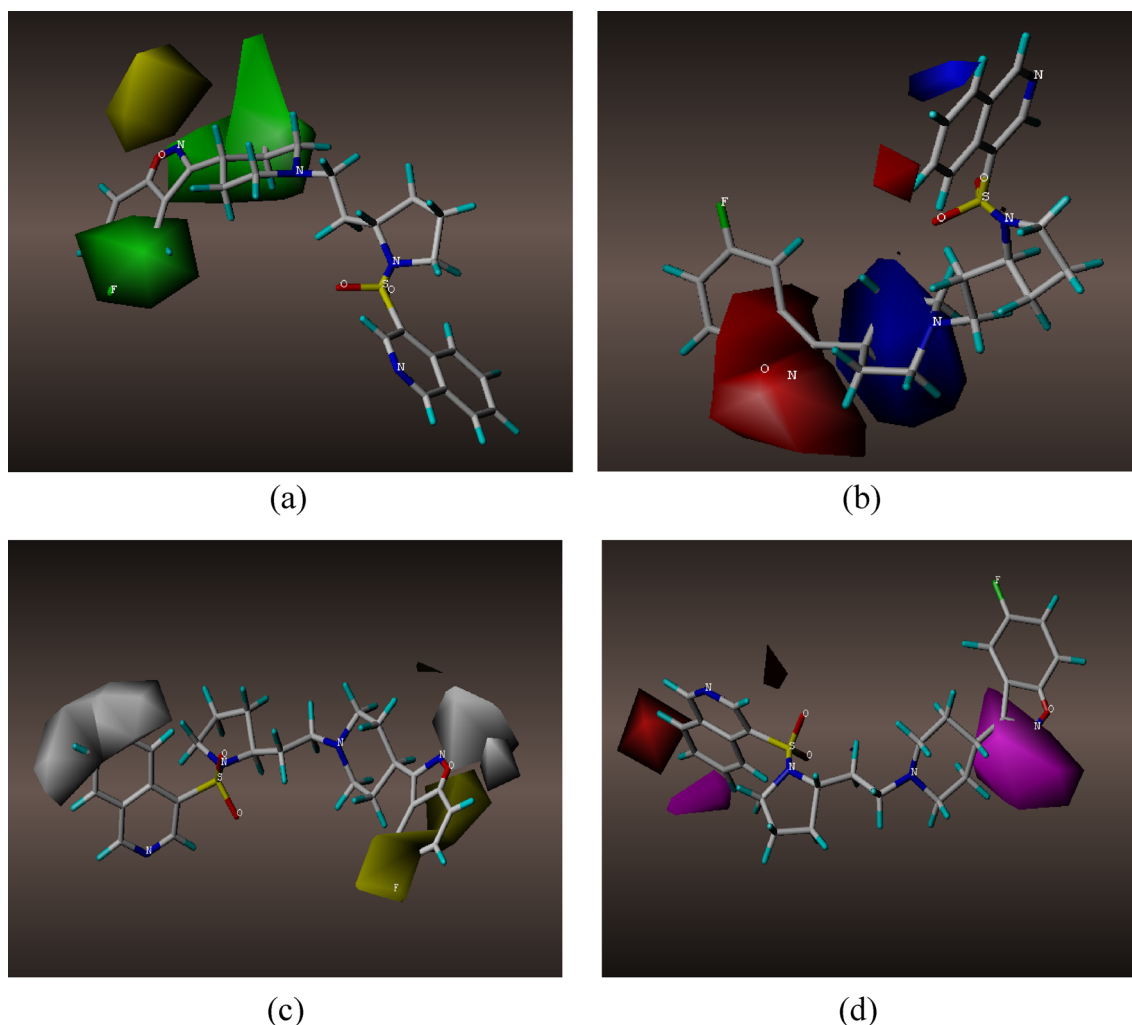


Fig. 6 Contour map analysis of 3D-QSAR model CoMSIA^a; Steric fields contribution (a); Electrostatic fields contribution (b); Hydrophobic fields contribution (c); H-bond acceptor groups (d)

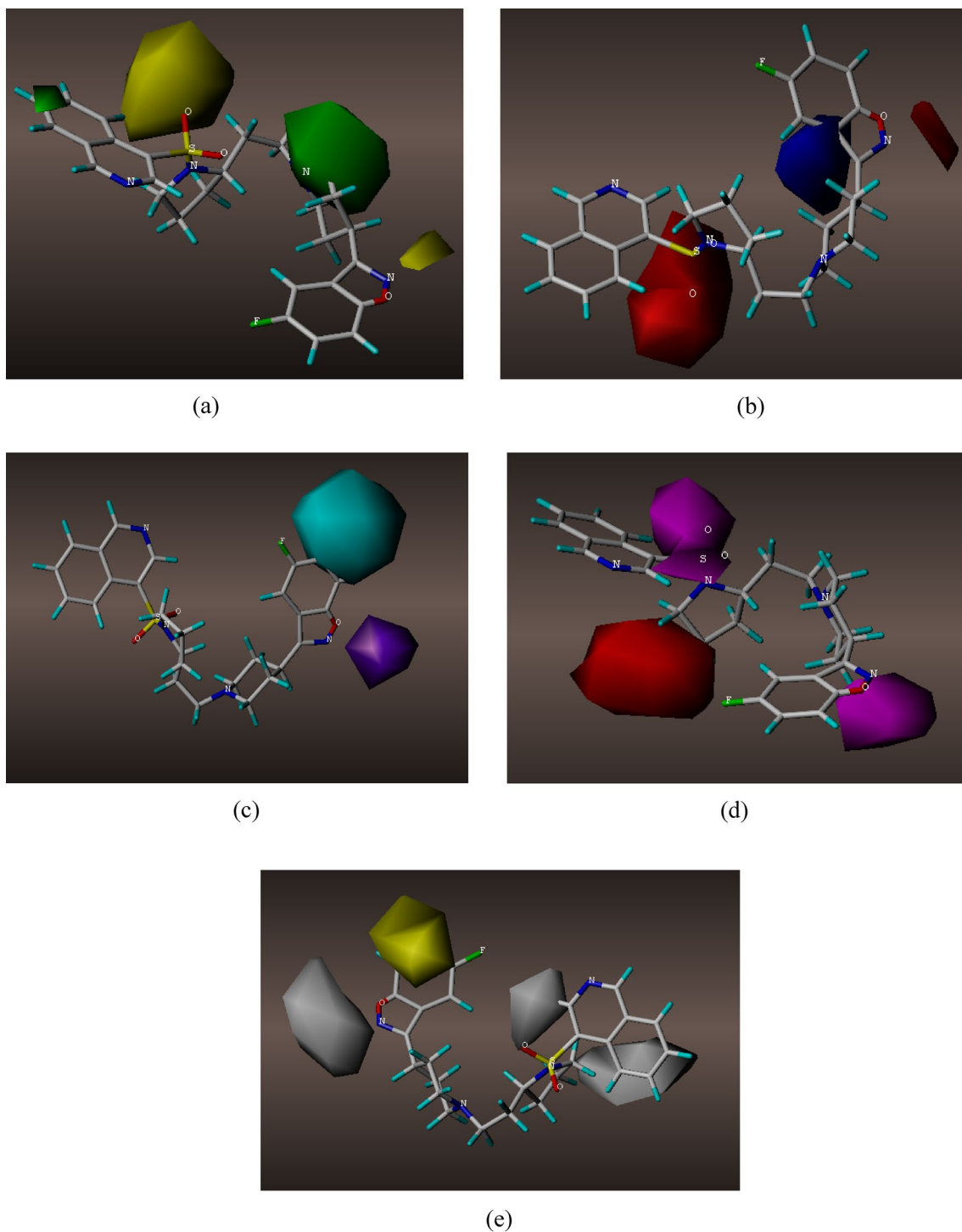


Fig. 7 Contour map analysis of 3D-QSAR model CoMSIA^b; Steric fields contribution (a); Electrostatic fields contribution (b); H-bond donor contribution (c); H-bond acceptor contribution (d); Hydrophobic fields contribution (e)

In the case of the CoMSIA^b model, the contour map of the most active ligand 6 h was structurally investigated for enhancing the biological activity against the D₂ receptor, by correlating their structure activity relationship. The steric, electrostatic, hydrophobic, H-bond donor and acceptor fields

have shown in Fig. 7. The steric contour (a) represented by the green contour map, suggested that steric bulkier groups are desired while the yellow color is unfavorable for steric substitution. The electrostatic contour (b) map, designated by blue color region around-benzo-(d)isoxazole moiety,

suggested that substitution of electropositive groups is favorable for activity. While red contour present near sulfonyl and pyrrolidine moiety suggested that substitution of electronegative groups may enhance the biological activity of the compound. The hydrogen bond donor contour (c) represented by cyan color indicated that substitution of H-bond donor over this region is favorable whereas the purple color region is unfavorable for H-bond donor substitution. The contour of H-bond acceptor (d) indicated by magenta color near nitrogen atom of pyrrolidine ring and isoxazole ring, suggested that substitution of H-bond acceptor in this region may enhance the receptor activity while red contour region is unfavorable for substitution. The yellow contour (e) is favorable for hydrophobic group substitution such as methyl group substitution can lead the biological activity, while the white color contour is an unfavorable region. The impact of the H-bond donor and acceptor contour map is a little bit lower for receptor antagonistic activity against

both the receptors. The major concern is steric and electrostatic group's contributions are the important substitution for improving the receptors' biological activity.

Optimization for new compounds

The CoMFA and CoMSIA based 3D-QSAR, virtual screening studies may be used for the design of new compounds towards schizophrenia. The structural activity relationship (SARs) of Azine sulfonamides of cyclic amine derivatives with different possible substituents is shown in Fig. 8 based on results obtained by the 3D-QSAR study. Here we can see the impact of the different substitution of groups may increase or decrease the activity of the receptor. Groups involved in substitution are electropositive, electronegative, H-bond acceptor, H-bond donor, hydrophobic, and steric bulky groups.

Fig. 8 Ligand scaffold with different features design by 3D-QSAR study for the development of novel compounds

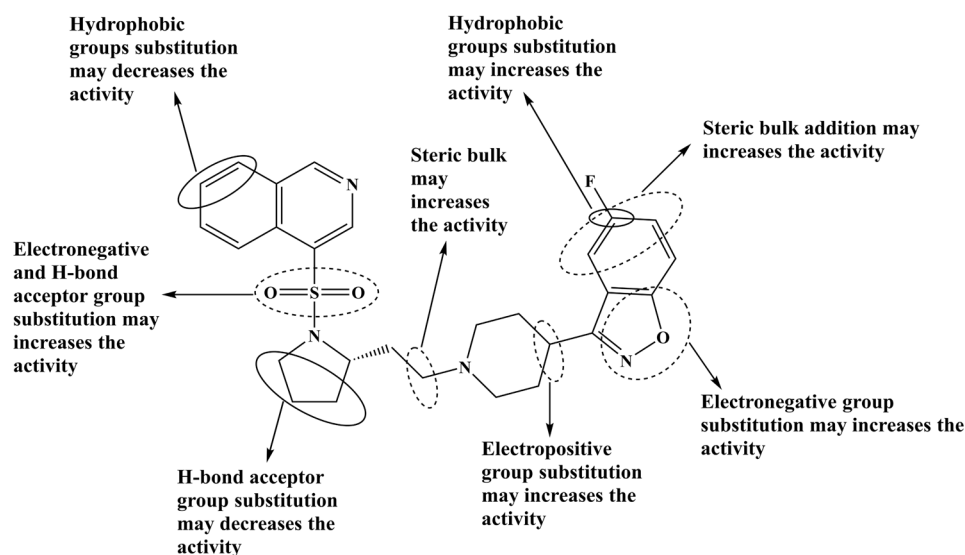
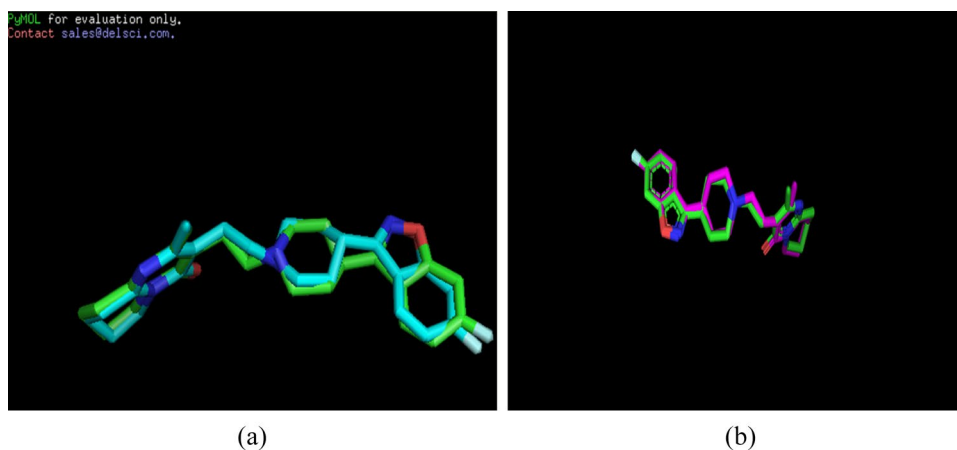


Fig. 9 a Superimposition of re-docked (sky-blue color) and co-crystallized (green color) ligand risperidone with 5-HT_{2A}R (PDB ID: 6A93) at 0.26 RMSD. **b** Superimposition re-docked (magenta color) and co-crystallized ligand risperidone (green color) with D₂R (PDB ID: 6CM4) at 0.24 RMSD



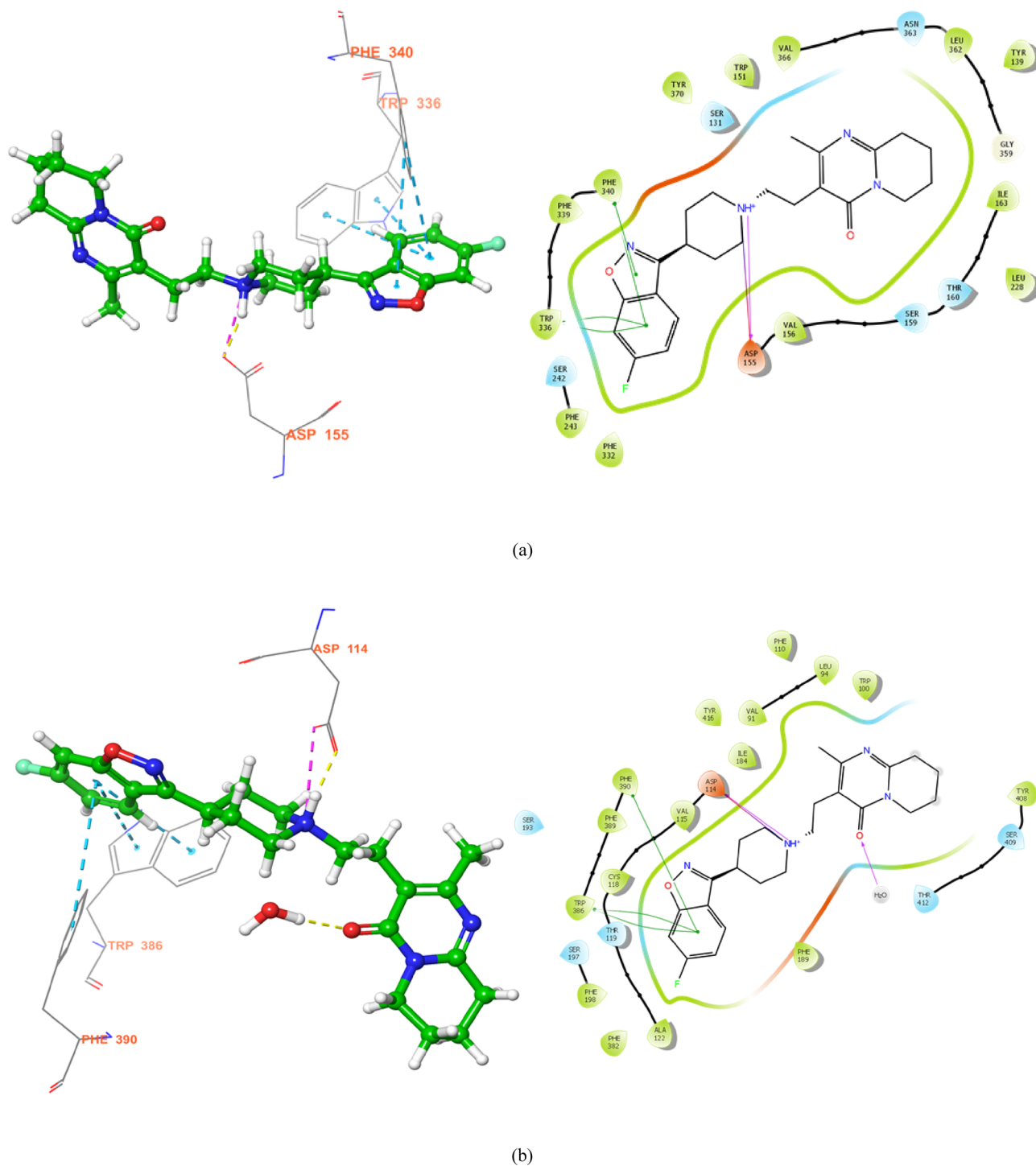


Fig. 10 Docking poses and 2D interaction diagram of template and compound 1 h against the receptors, **a** Template, PDB ID: 6A93; **b** Template, PDB ID: 6CM4; **c** Compound 1 h, PDB ID: 6A93; **d** Compound 1 h, PDB ID: 6CM4

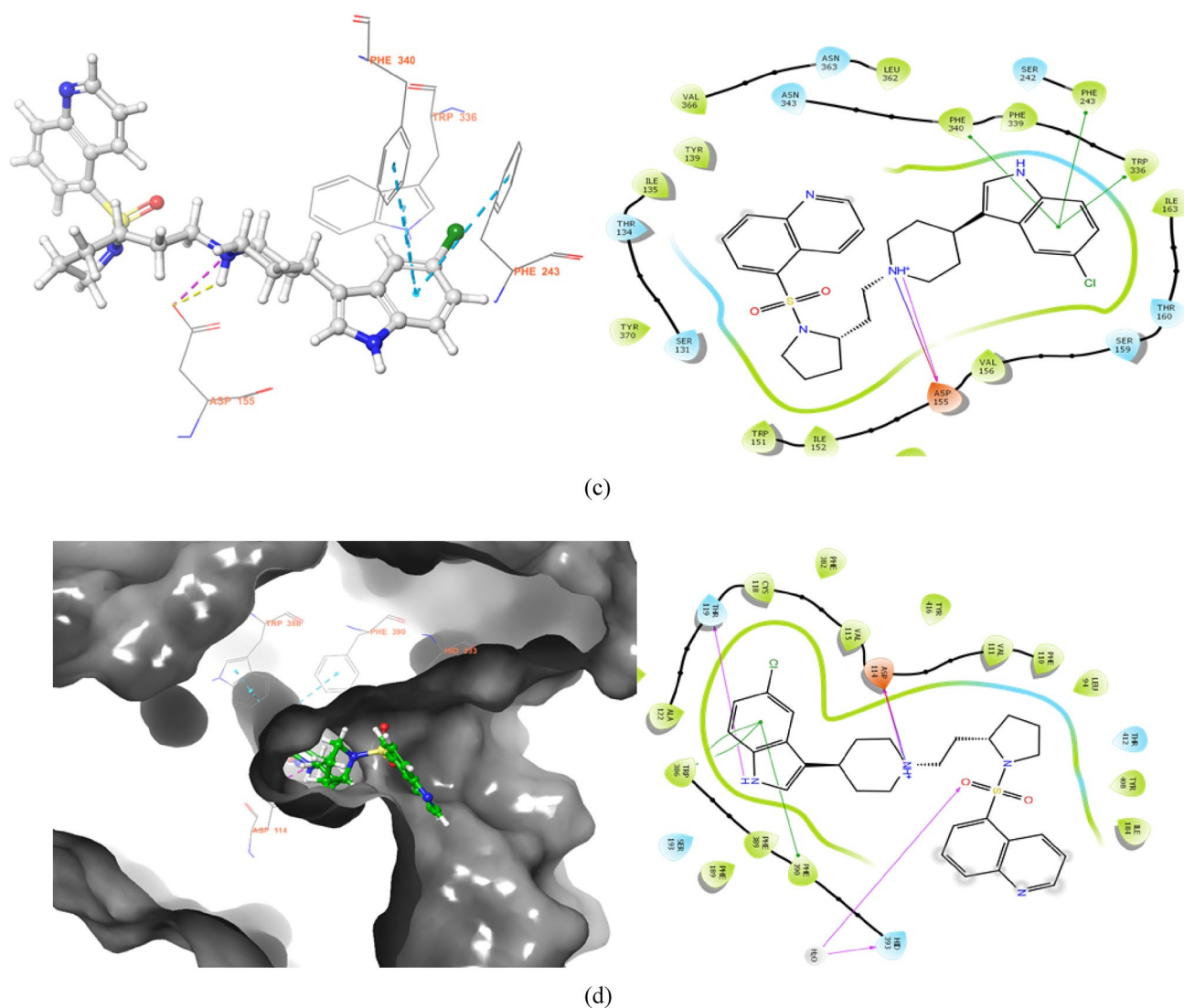


Fig. 10 (continued)

Molecular docking

Molecular docking is performed using the maestro 5.2 Schrödinger module. The method is most common for finding and identifying the binding interaction between the ligands and receptors. The method is validated by superimposing of both re-docked and co-crystallized ligand risperidone (Fig. 9) with the help of Pymol (Vs 2.3.3) and corresponding RMSD was calculated. The RMSD values between both docked conformations were 0.26 for 5-HT_{2A} and 0.24 for the D₂ receptor. The low value of RMSD validates the robustness and reliability of the docking procedure.

The 5-HT_{2A} receptor is a G-protein coupled receptor having seven transmembrane helices (TM1-7) and an intracellular amphipathic helix H8 in the domains of TM-4, an extended cavity that is connected to the orthosteric site. The

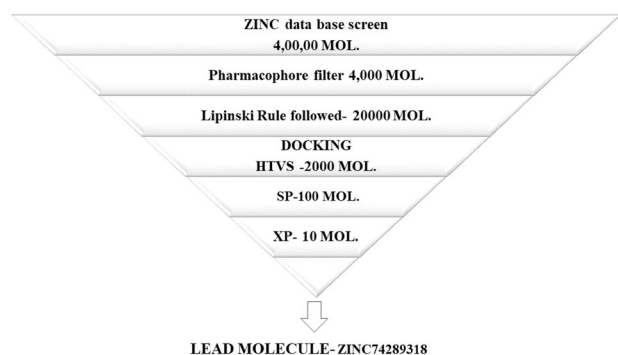
fragment pocket (PIF) consists of amino acids as Ile163 and Phe332 and the interaction with the toggle switch residue **Trp336** is a must for the receptor activation and pharmacological action.

Risperidone was used as a co-crystallized ligand to analyze the binding orientations of different ligands to 5-HT_{2A}R and D₂R. Figure 10a, b represent the binding interaction of co-crystallized ligand having Van der Waals and hydrophobic interaction with the key residues like Trp336, Asp155, and Phe340, other important residues are Leu229, Asn343, and Phe339 for 5-HT_{2A}R. In the case of D₂R, the key structural amino acid residues are Asp114, Trp386, Phe390, and one water molecule. Here, Trp386 amino acid residue is playing a key role in the partial activation of this receptor.

Among all the compounds in the data set, compound **1 h** showed a good docking score. All the compounds possess

Table 6 Summary of docking study (by using XP Methodologies) results with their crucial binding cavity, interaction residues

Name of ligand	Amino acid residue	H-bond	Pi-Pi stacking	Pi-cation	Salt bridge	Docking Score (xp) kcal/mol	Receptor ID
1 h	ASP155	Yes	No	No	Yes	− 8.734	6A93
	PHE243	No	Yes	No	No		
	PHE340	No	Yes	No	No		
	TRP336	No	Yes	No	No		
ZINC74289318	ASP155	Yes	No	No	Yes	− 10.744	6A93
	LEU229	Yes	No	No	No		
	ASN343	Yes	No	No	No		
	PHE340	No	Yes	No	No		
	PHE339	No	Yes	No	No		
	TRP336	No	Yes	No	No		
	TRP336	No	Yes	No	No		
Risperidone	ASP155	Yes	No	No	Yes	− 8.40	6A93
	PHE340	No	Yes	No	No		
	TRP336	No	Yes	No	No		
D₂ Receptor							
1 h	ASP114	Yes	No	No	Yes	− 8.268	6CM4
	THR119	Yes	No	No	No		
	TRP386	No	Yes	No	No		
	PHE390	No	Yes	No	No		
	HID393-H ₂ O	Yes	No	No	No		
ZINC74289318	ASP114	Yes	No	No	Yes	− 11.388	6CM4
	TRP386	No	Yes	No	No		
	PHE390	No	Yes	No	No		
	HID393-H ₂ O	Yes	No	No	No		
Risperidone	ASP114	Yes	No	No	Yes	− 10.086	6CM4
	TRP386	No	Yes	No	No		
	PHE390	No	Yes	No	No		
	PHE390	No	Yes	No	No		
	H ₂ O	Yes	No	No	No		

**Fig. 11** Flow chart of virtual screening methods

piperidine or piperazine rings which contain a protonizable nitrogen atom, play an important role in hydrogen bonding with the binding cavity residue Asp115 of 5-HT_{2A} and residue Asp114 of D₂R. Compound 1 h showed Pi-Pi stacking with amino acid residues like Trp336, Phe340, Phe243, and Phe339 against 5-HT_{2A}R while Trp386 and Phe390 against

D₂R. The Pi-Pi stacking interaction depends on the heterocyclic ring attached to the piperidine and piperazine motif. Ex. 1 h having (5-chloro-1H indole-3yl) and 6 h having benzo-(d)isoxazole, an important moiety forming hydrophobic interactions. The binding cavity of potent ligands with their interactive amino acid residues are represented with the help of the 2D interactions diagram shown in Fig. 10c, d. The docking interactions and scoring results of the best compounds were shown in Table 6.

Virtual screening and docking

The docking-based virtual screening was carried out using selected pharmacophore hypotheses AAHPRRR_1. Based on the selected pharmacophore hypotheses features, the ZINC database was screened by applying filters criteria like Lipinski rule of five, Rotatable bond, and maximum RMSD selected 2 for hits screening. The HTVS, SP, and XP docking methods were carried out to find out the lead molecule from the database. The ligand **ZINC74289318** obtained as a

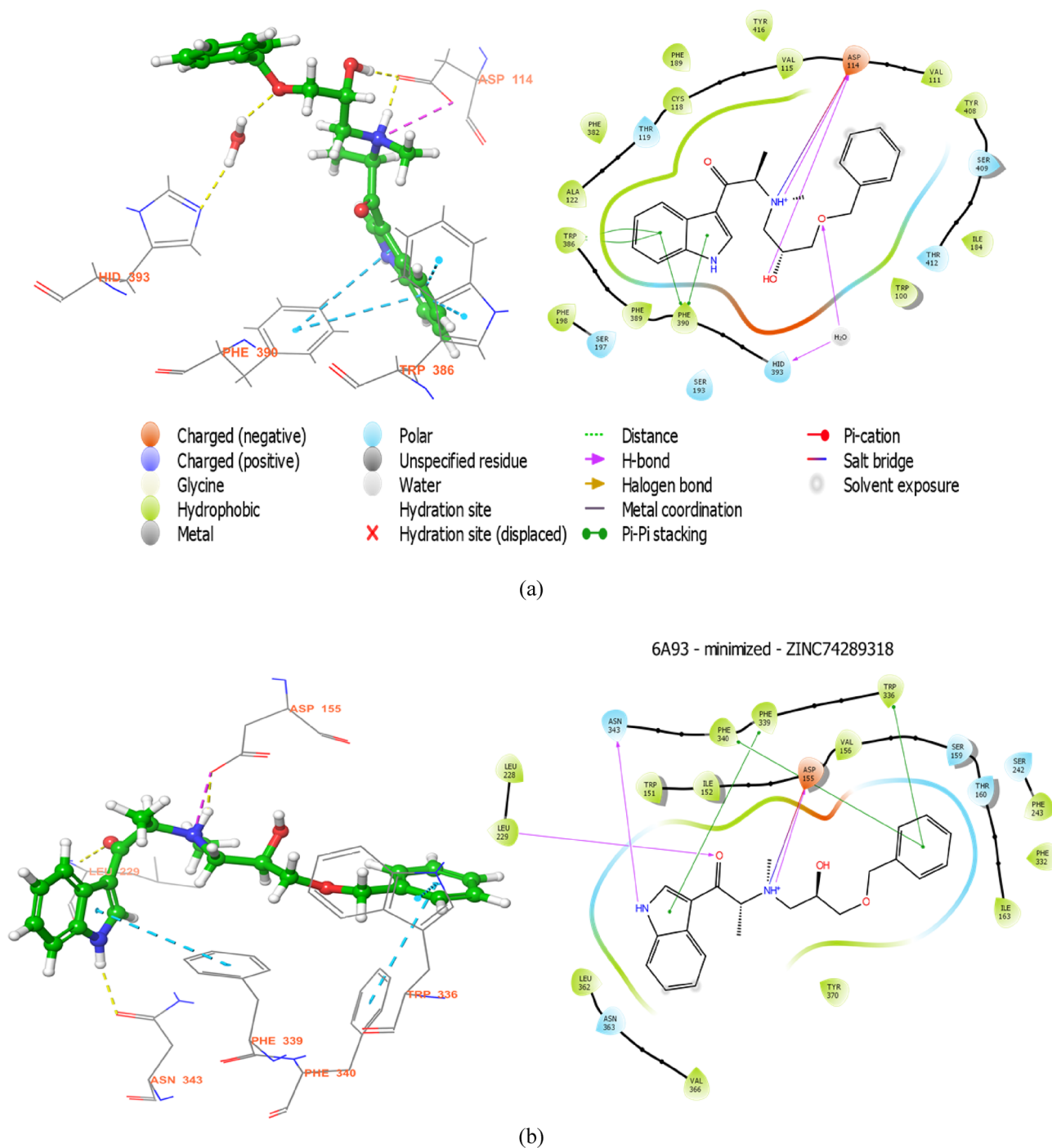
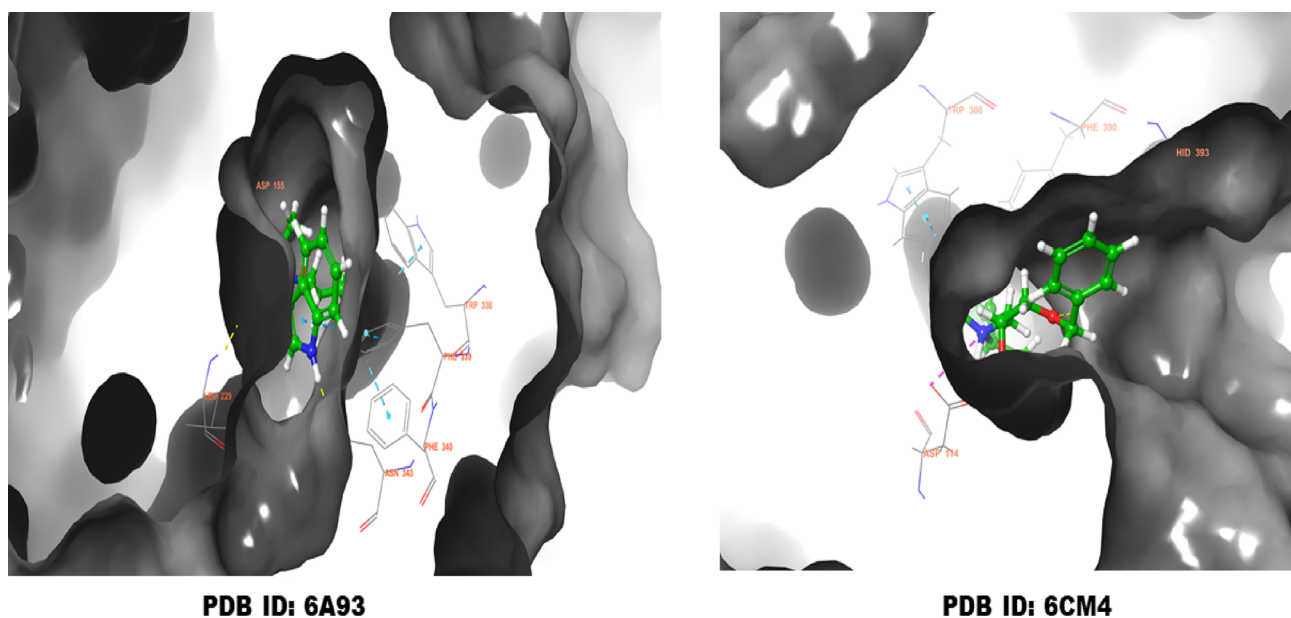


Fig. 12 3D-Docking results with 2D interaction diagrams of higher scoring compound ZINC74289318; D₂R (a); 5-HT_{2A}R (b); Binding cavity of both the receptors (c); Chemical structure (d)

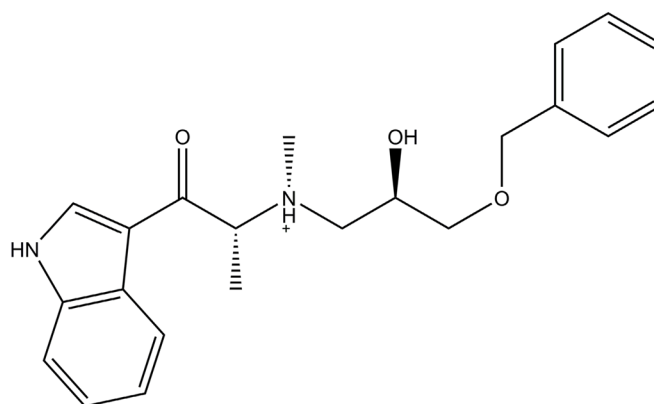
lead molecule showed a very promising binding interaction and docking score shown in Table 6. The methods of virtual screening are represented diagrammatically in Fig. 11.

Compound ZINC74289318 was considered as a lead molecule for the recent study, based on results. The compound

showed higher docking score and better binding interactions into the binding cavity than co-crystallized ligand for both the receptors, which enhanced the selectivity of the ligand toward its receptors. Compound ZINC74289318 having two additional hydrogen bonds and one additional Pi-Pi stacking



(c)



(d)

Fig. 12 (continued)

with amino acid residues LEU229, ASN343, and PHE339 respectively, which are responsible for the antagonistic effect of 5-HT_{2A}R crystal ID: 6A93. In the case of D₂R, the compound showed one additional hydrogen bond between the hydroxy group (attached to benzyloxy and N-methylpropane) and amino acid residue ASP114. The ZINC ligand has a unique quaternary amine (aminium ion), which is responsible for receptors inhibitory activity, rather than piperazine and piperidine ring bearing nitrogen atoms. The 3D poses of docking results and 2D interaction diagram of compound ZINC74289318 for both the targets are shown in Fig. 12.

Absorption, distribution, metabolism, excretion, and toxicity predictions

Based on active pharmacophoric features, binding mechanism, and docking scores, molecules were selected for their ADME properties prediction. ADME properties of the lead compound were calculated by using online SwissADME software (Fig. 13). The parameter for drug-likeness or as drug candidate was found to be within the acceptable limit for the topmost selected one as ZINC hits (Table 7). The ZINC compound ZINC74289318 showed that it passes the drug-likeness parameter without violating any rules. Also, the bioavailability score is 0.55 which is a significant value

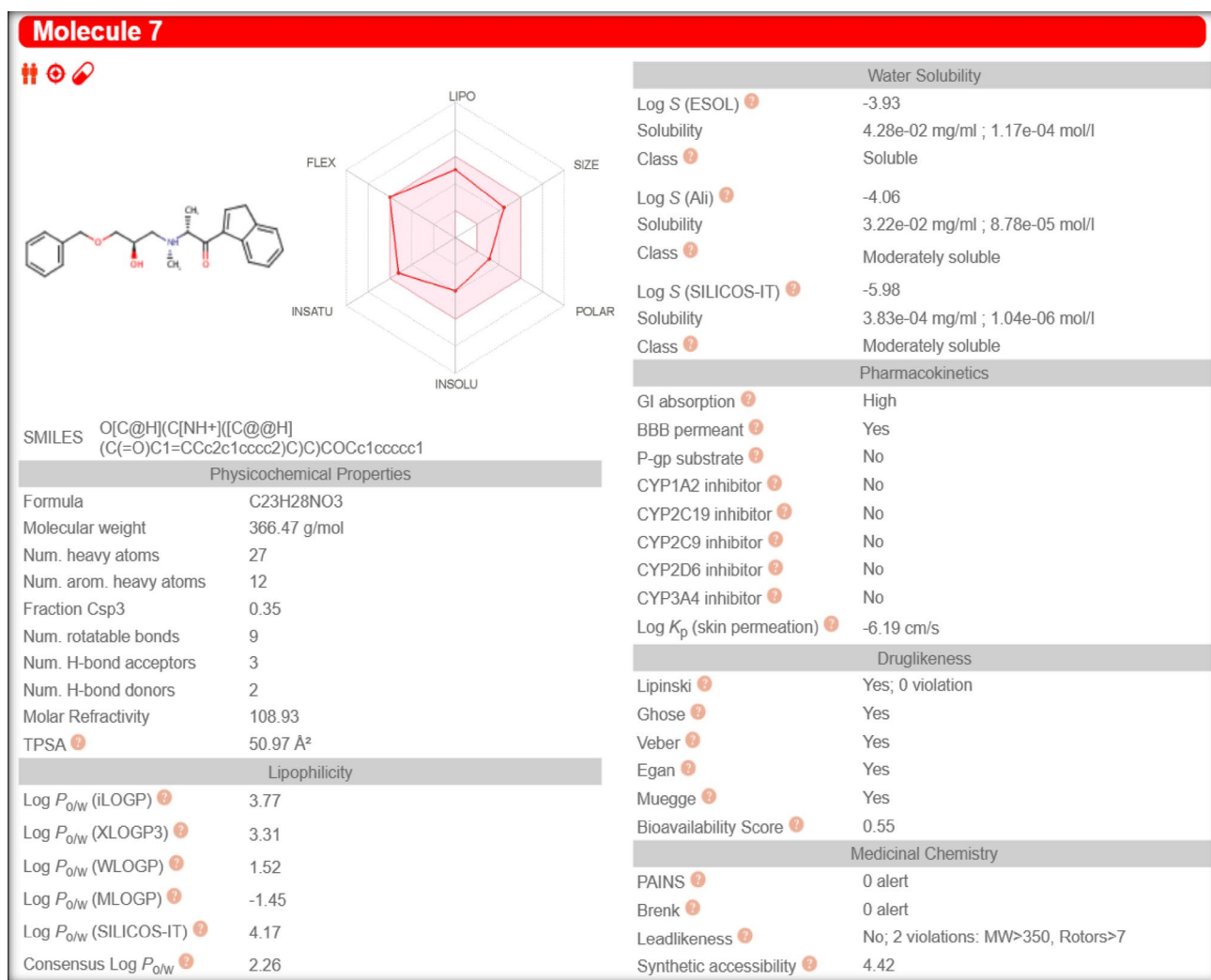


Fig. 13 ADMET results of ZINC74289318

Table 7 ADME prediction of ZINC hit and standard drug by using SwissADME online tool

S. no	Compound name	Mol. Wt. (g/mol)	Molar refractivity	GI absorption	BBB permeability	Log P _{0/w}	Solubility	Synthetic Accessibility
1	1 h	523.09	153.65	High	Yes	5.28	Poorly	4.38
2	ZINC74289318	366.47	108.93	High	Yes	3.31	Soluble	4.42
3	Risperidone	410.48	117.71	High	Yes	2.78	Moderately	4.27

Table 8 Toxicity prediction of ZINC74289318 and ligand 1 h and reference drug by using SwissADME online tool

S. no	Compound name	CYP1A2	CYP2C19	CYP2C9	CYP2D6	CYP3A4	Pgp substrate
1	1 h	No	Yes	Yes	Yes	Yes	Yes
2	ZINC74289318	No	No	No	No	No	No
3	Risperidone	No	Yes	Yes	Yes	Yes	Yes

for a drug candidate. The synthetic accessibility of the compound was dominant than the co-crystallize.

The molecule also showed good GI absorption and blood–brain barrier permeability, the solubility parameter suggested that its solubility is better than co-crystallized ligand. Also, it does not act as a substrate of P-gp. Similarly, it has no inhibitory and toxic effect on the enzyme of cytochrome P450 (CYP1A2, CYP2C19, CYP2C9, CYP2D6, and CYP3A4) Table 8. The $\text{Log}_{\text{p}/\text{w}}$ is 3.31 which is good value for considering the lipophilicity of ligand.

The predicted ADME properties of the ligand **1 h** showed good results with some drawbacks having poor solubility, high molar refractivity. It also showed a higher molecular weight that more than 500 g/mol, which causes a violation of the Lipinski rule of five. The compound has inhibited the enzyme of cytochrome P450 (CYP1A2, CYP2C19, CYP2C9, CYP2D6, and CYP3A4), which may lead to adverse effects.

The SwissADME study profile of compounds suggested that the major concern is to reduce the molecular weight, improve compound lipophilicity and molar refractivity of compounds.

Conclusion

The present study reveals the computational design of compounds bearing antipsychotic activity against 5-HT_{2A} and D₂ receptors. A series of azinesulphonamide derivatives as dual receptor antagonists was used for in silico studies including QSAR, molecular docking, pharmacophore model, and ADME prediction. The pharmacophore hypothesis study was performed by using the PHASE module. The developed hypothesis was ranked based on their different scoring function. The best hypothesis was AAHPRRR_1 selected from the study.

The best 3D-QSAR models showed high regression coefficient for the training ($R^2 > 0.893$; 0.820) and test ($Q^2 > 0.552$; 0.577) sets for both 5-HT_{2A} and D₂ receptors respectively. The developed models were validated by internal and external validation parameters which showed significance. Contour maps concerning compounds suggest different structural insights determined by the electrostatic, hydrophobic, H-bond donor, H-bond acceptor, and steric fields. The compound **1 h** showed docking scores – 8.734, – 8.268 kcal/mol with XP docking modes, consecutively, against 5-HT_{2A} (PDB ID: 6A93) and (PDB ID: 6CM4) receptor. The pharmacophore model was further used to screened molecules from the ZINC molecules database. These molecules were processed through a virtual screening study from Schrodinger virtual screening module. The HTVS, SP, and XP methodologies were used for screening the top best-docked hit compound ZINC74289318 complex of both the receptors showed promising docking

score (– 10.74 kcal/mol for 5-HT_{2A}; – 11.388 kcal/mol for D₂R) and binding interaction. Molecular docking revealed that quaternary or protonizable nitrogen atoms on piperidine and piperazine rings showed a hydrogen bond that directly affected the receptor activity. The important hydrophobic amino acid residues, TRP336, PHE340, PHE339 of 5-HT_{2A}R, and TRP386, PHE390 of D₂R, were vital elements in the stability of the antagonist binding site. The pharmacokinetic properties were also calculated for the dataset, reference molecule, and ZINC hits using SwissADME tools. Only ZINC hits and the co-crystallized ligand pass all the parameters without any violation. The overall ADMET parameters like blood–brain barrier permeability, GI absorption, solubility, toxicity, and bioavailability showed that compound ZINC74289318 has high GI absorption, high blood–brain barrier permeability, good lipophilicity having $\text{Log } P_{\text{o}/\text{w}}$ 3.31, synthetic accessibility value 4.42 (greater than risperidone), and follow Lipinski rule of five with zero violation of drug-like criteria. The overall computational studies concluded that Docking, 3D QSAR, Pharmacophore modeling, and ADMET prediction are very helpful to suggest and design a novel hit compound for antipsychotic activity. Furthermore, this study will provide direction to researchers to design novel piperazine and piperidine derivatives as antipsychotic agents.

Acknowledgements Akash Rathore is thankful to the All India Council for Technical Education (AICTE), New Delhi for awarding fellowship. Authors acknowledge the Department of Pharmaceutical Sciences, Dr. Harisingh Gour University (A Central University), India for providing research facilities.

Funding The work was done under the All India Council for Technical Education (AICTE) fellowship for GPAT with reference no AICTE-2018–00000472.

Declarations

Conflict of interest Authors declare no conflict of interest.

References

- Abdizadeh R, Hadizadeh F, Abdizadeh T (2020) QSAR analysis of coumarin-based benzamides as histone deacetylase inhibitors using CoMFA, CoMSIA and HQSAR methods. *J Mol Struct* 1199:126961
- Butini S, Gemma S, Campiani G, Franceschini S, Trotta F, Borriello M, Ceres N, Ros S, Coccone SS, Bernetti M, De Angelis M (2008) Discovery of a new class of potential multifunctional atypical antipsychotic agents targeting dopamine D₃ and serotonin 5-HT_{1A} and 5-HT_{2A} receptors design, synthesis, and effects on behavior. *J Med Chem* 52(1):151–169
- Cao X, Zhang Y, Chen Y, Qiu Y, Yu M, Xu X, Liu X, Liu BF, Zhang L, Zhang G (2018) Synthesis and biological evaluation of fused tricyclic heterocycle piperazine (Piperidine) derivatives as potential multireceptor atypical antipsychotics. *J Med Chem* 61(22):10017

- Daina A, Michielin O, Zoete V (2017) SwissADME: a free web tool to evaluate pharmacokinetics, drug-likeness and medicinal chemistry friendliness of small molecules. *Sci Rep* 7:42717
- Dixon L, Smondyrev AM, Knoll EH, Rao SN, Shaw DE, Friesner RA (2006) PHASE: a new engine for pharmacophore perception, 3D QSAR model development, and 3D database screening: 1. Methodology and preliminary results. *J Comp Aid Mol Des* 20(10–11):647–671
- Ghaleb A et al (2017) 3D-QSAR modeling and molecular docking studies on a series of 2, 5 disubstituted 1, 3, 4-oxadiazoles. *J Mol Struct* 1145:278–284
- Ghasemi JB, Shiri F (2012) Molecular docking and 3D-QSAR studies of falcipain inhibitors using CoMFA, CoMSIA, and Open3DQSAR. *Med Chem Res* 21(10):2788–2806
- Huang L, Zhang W, Zhang X, Yin L, Chen B, Song J (2015) Synthesis and pharmacological evaluation of piperidine (piperazine)-substituted benzoxazole derivatives as multi-target antipsychotics. *Bioorg Med Chem Lett* 25(22):5299–5305
- Jaiteh M et al (2020) Performance of virtual screening against GPCR homology models: impact of template selection and treatment of binding site plasticity. *PLoS Comput Biol* 16.3:e1007680
- Kapur SR (2001) Gary Atypical antipsychotics new directions and new challenges in the treatment of schizophrenia. *Annu Rev Med* 52(1):503–517
- Kimura KT et al (2019) Structures of the 5-HT_{2A} receptor in complex with the antipsychotics risperidone and zotepine. *Nat Struct Mol Biol* 26.2(2019):121–128
- Klebe G, Abraham U, Mietzner T (1994) Molecular similarity indices in a comparative analysis (CoMSIA) of drug molecules to correlate and predict their biological activity. *J Med Chem* 37(24):4130–4146
- Kumar A, Singh H, Mishra A, Mishra AK (2018) Aripiprazole: an FDA approved bioactive compound to treat schizophrenia—a mini review. *Curr Drug Discov Technol* 17(1):23–29
- Lee JH, Sung JC, Mi-hyun K (2018) Discovery of CNS-like D₃R-selective antagonists using 3D pharmacophore guided virtual screening. *Molecules* 23.10(2018):2452
- Leucht S, Kissling W, Davis JM (2009) Second-generation antipsychotics for schizophrenia can we resolve the conflict. *Psychol Med* 39(10):1591–1602
- Liddle PF (1987) Schizophrenic syndromes, cognitive performance, and neurological dysfunction. *Psychol Med* 171:49–57
- McCutcheon RA, Marques TR, Howes OD (2020) Schizophrenia—an overview. *JAMA Psychiat* 2:201–210
- Modugula H, Kumar A (2020) Risk analysis of lurasidone in patients with schizophrenia and bipolar depression, CNS and neurological disorders-drug targets (formerly current drug targets-CNS and neurological disorders).
- Murthy VS, Vithal MK (2002) 3D-QSAR CoMFA and CoMSIA on protein tyrosine phosphatase 1B inhibitors. *Bioorg Med Chem* 107:2267–2282
- Oprea TI et al (2001) MTD-PLS: A PLS-based variant of the MTD method. A 3D-QSAR analysis of receptor affinities for a series of halogenated dibenzoxin and biphenyl derivatives. *SAR QSAR Environ Res* 12.1–2:75–92
- Peprah K, Zhu XY, Eyunni SV, Setola V, Roth BL, Ablordeppey SY (2012) Multi-receptor drug design Haloperidol as a scaffold for the design and synthesis of atypical antipsychotic agents. *Bioorg Med Chem* 20(3):1291–1297
- Rajeswari M, Santhi N, Bhuvanewari V (2014) Pharmacophore and virtual screening of JAK3 inhibitors. *Bioinfo* 10(3):157–163
- Rossler W, Salize HJ, van Os J, Riecher-Rossler A (2005) Size of burden of schizophrenia and psychotic disorders. *Eur Neuropsychopharmacol* 15:399–409
- Verma J, Khedkar VM, Coutinho EC (2010) 3D-QSAR in drug design—a review. *Curr Top Med Chem* 10(1):95–115
- Wang S, Che T, Levit A, Shoichet BK, Wacker D, Roth BL (2018) Structure of the D₂ dopamine receptor bound to the atypical antipsychotic drug risperidone. *Nature* 555(7695):269–273
- Wood DJ et al (2012) Pharmacophore fingerprint-based approach to binding site subpocket similarity and its application to bioisostere replacement. *J Chem Inform Model* 52.8:2031–2043
- Xiamuxi H, Wang Z, Li J, Wang Y, Wu C, Yang F, Jiang X, Liu Y, Zhao Q, Chen W, Zhang J (2017) Synthesis and biological investigation of tetrahydropyridopyrimidinone derivatives as potential multireceptor atypical antipsychotics. *Bioorg Med Chem* 19(10):4904–4916
- Xu M, Wang Y, Yang F, Wu C, Wang Z, Ye B, Jiang X, Zhao Q, Li J, Liu Y, Zhang J (2018) Synthesis and biological evaluation of a series of novel pyridinecarboxamides as potential multi-receptor antipsychotic drugs. *Bioorg Med Chem Lett* 76(5):606–611
- Zajdel P, Kos T, Marciniak K, Satała G, Canale V, Kamiński K, Hołuj M, Lenda T, Koralewski R, Bednarski M, Nowiński L (2018) Novel multi-target azinesulfonamides of cyclic amine derivatives as potential antipsychotics with pro-social and pro-cognitive effects. *Eur J Med Chem* 145:790–804
- Zhang C et al (2020) Design of novel dopamine D₂ and serotonin 5-HT_{2A} receptors dual antagonists toward schizophrenia: An integrated study with QSAR, molecular docking, virtual screening, and molecular dynamics simulations. *J Biomol Struct Dyn* 383:860–885

Publisher's Note Springer Nature remains neutral with regard to jurisdictional claims in published maps and institutional affiliations.